

Motion Error Compensation Method for Hydrostatic Tables Using Actively Controlled Capillaries

Chun Hong Park*, **Yoon Jin Oh**, **Joo Ho Hwang**

*Intelligent Machine Systems Center, Korea Institute of Machinery & Materials,
171, Jang-dong, Yuseong-gu, Daejeon 305-343, Korea*

Deug Woo Lee

*Nano Science and Technology Faculty, Pusan National University,
Busan 609-735, Korea*

To compensate for the motion errors in hydrostatic tables, a method to actively control the clearance of a bearing corresponding to the amount of error using actively controlled capillaries is introduced in this paper. The design method for an actively controlled capillary that considers the output rate of a piezo actuator and the amount of error that must be corrected is described. The basic characteristics of such a system were tested, such as the maximum controllable range of the error, micro-step response, and available dynamic bandwidth when the capillary was installed in a hydrostatic table. The tests demonstrated that the maximum controllable range was $2.4 \mu\text{m}$, the resolution was 27 nm , and the frequency bandwidth was 5.5 Hz . Simultaneous compensation of the linear and angular motion errors using two actively controlled capillaries was also performed for a hydrostatic table driven by a ballscrew and a DC servomotor. An iterative compensation method was applied to improve the compensation characteristics. Experimental results showed that the linear and angular motion errors were improved to $0.12 \mu\text{m}$ and 0.20 arcsec , which were about $1/15^{\text{th}}$ and $1/6^{\text{th}}$ of the initial motion errors, respectively. These results confirmed that the proposed compensation method improves the motion accuracy of hydrostatic tables very effectively.

Key Words : Actively Controlled Capillary, Hydrostatic Bearing Table, Error Compensation, Linear Motion Error, Angular Motion Error

1. Introduction

The motion accuracy of an ultra-precision feed table is mainly affected by the machining accuracy of the guide rail. In most cases, a lapping process is introduced since the required accuracy cannot be achieved using only a ground guide rail. However, as this process largely depends on

the skills of a craftsman, improved productivity and a more systematized manufacturing process cannot be obtained.

Recently, active control techniques have been widely attempted to develop ultra-precision feed tables without the aid of a skilled craftsman. An ultra-precision straight motion system using active air bearings composed of PZT actuators and air pads was proposed (Aoyama et al., 1988). The active air bearings improved the accuracy of the linear and angular motions to $0.14 \mu\text{m}$ and 0.14 arcsec . An active inherent restrictor was also introduced, consisting of a PZT actuator with a hole functioning as an orifice that actively controlled the air bearing clearance (Mizumoto et al., 1996). It showed that the rotational accuracy of

* Corresponding Author,

E-mail : pch657@kimm.re.kr

TEL : +82-42-868-7117; **FAX :** +82-42-868-7180

Intelligent Machine Systems Center, Korea Institute of Machinery & Materials, 171, Jang-dong, Yuseong-gu, Daejeon 305-343, Korea. (Manuscript **Received** April 11, 2005; **Revised** December 17, 2005)

an air spindle in the radial direction could be improved from $0.2 \mu\text{m}$ to $0.02 \mu\text{m}$ using a feedback control consisting of six active inherent restrictors and two displacement sensors. These studies demonstrated that the motion accuracy of an ultra-precision table could be improved without using conventional precision machining processes that depend on a craftsman's skill. However, some difficulties were encountered, since the error compensation system had to be machined inside the ultra precision bearing and a in-process feedback control system installed.

One way to improve the motion accuracy of hydrostatic tables without changing the bearing structure or installing a in-process feedback control system is to use an actively controlled capillary (ACC). In an ACC, the clearance of an annular capillary is actively controlled using a piezo actuator. Then, by the followed variation of pocket pressure, the clearance of double-sided hydrostatic pad is adjusted as required. Linear and angular motion errors can be corrected simultaneously using successive control by measuring the size of each error using two ACCs. Since this compensation method is performed using an open loop process, the process can be iterated until the motion accuracies does not further improve. Also, an additional device mounted inside the structure for in-process control is not needed. Therefore it provides a great advantage to make it practical in the aspect of stabilization of performance in the spatial case as well.

This paper describes the theoretical design procedure of an ACC and tests of its basic characteristics, such as the maximum controllable

range, micro-step response, and available dynamic bandwidth. An iterative compensation method was applied to improve the accuracy of the compensation (Hageman and Young, 1981). To verify the effectiveness of the motion error compensation method, simultaneous compensation of the linear and angular motion errors of a hydrostatic table driven by a ballscrew and a DC servomotor was performed using two ACCs.

2. Actively Controlled Capillaries

The structure of the proposed ACC is shown in Fig. 1. It consists of three main parts : the upper body, lower body, and circular leaf spring pad, which is inserted between the upper and lower bodies. The tolerance between the bottom of the cylindrical oil inlet and the surface of the leaf spring comprises the clearance of an annular capillary; this clearance is varied by the displacement of a piezo actuator placed under the leaf spring.

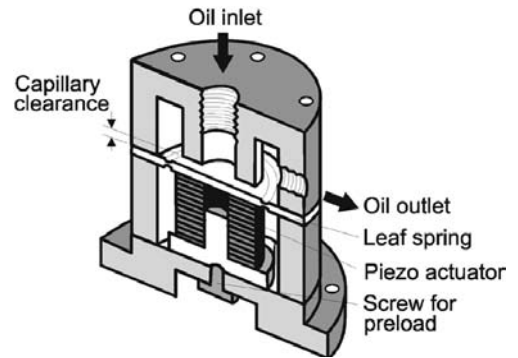


Fig. 1 Features of an actively controlled capillary

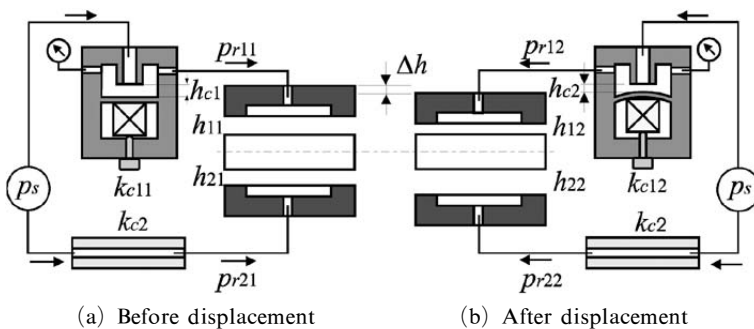


Fig. 2 Operating principles of an actively controlled capillary

The operating principle of the ACC is illustrated in Fig. 2. In order to correct the motion error of a double-sided hydrostatic table, an ACC is connected to one side while a traditional fixed-length capillary is connected to the other side. After applying an excitation voltage $E(x)$ to the piezo actuator, the clearance of the ACC decreases from h_{c1} to h_{c2} . The decreased flow rate owing to the change in clearance results in a decrease of the pocket pressure p_{r11} . Consequently, the table moves downward with a displacement of Δh . Therefore, the motion error can be improved by using successive control corresponding to the position of the table on the guide rail. In practical applications, there exist linear and angular error components. Therefore, two ACCs are used together. In this case, the excitation voltages $E_1(x)$ and $E_2(x)$ supplied to the piezo actuators of each ACC can be calculated from

$$\begin{pmatrix} E_2(x) \\ E_2(x) \end{pmatrix} \begin{bmatrix} G_1 & 0 \\ 0 & G_2 \end{bmatrix} \begin{bmatrix} 1 & a \\ 1 & -a \end{bmatrix} \begin{pmatrix} K_z z(x) \\ K_\theta \theta(x) \end{pmatrix} \quad (1)$$

where x is the coordinate of the table center in the feed direction, a is the distance between the table center and the center of the pocket connected to the ACC, $z(x)$ and $\theta(x)$ are the measured linear and angular motion errors, G_i is the gain of the ACCs, and K_z and K_θ are the linear and angular compensation coefficients used to improve the converging characteristics of the iterative compensation method.

3. Design of the ACC

The inflow Q_{in} and outflow Q_{out} of a single-sided hydrostatic bearing with a capillary compensator are

$$Q_{in} = \frac{k_c}{\eta} (p_s - p_r), \quad Q_{out} = \frac{\bar{B} h_0^3}{\eta} p_r \quad (2)$$

where the pocket pressure p_r inside the bearing is calculated from the continuity condition of the flow (Aoyama, 1990).

$$p_r = \frac{1}{1 + \xi_0} p_s, \quad \xi_0 = \frac{\bar{B} h_0^3}{k_c} \quad (3)$$

and p_s is the supply pressure, k_c is the capillary coefficient, η is the viscosity of the oil, \bar{B} is a flow coefficient that depends only on the pad dimensions (Sharma et al., 2002), h_0 is the bearing clearance, and ξ_0 is the resistance ratio (Canbulut et al., 2004) of the capillary to the land of the bearing.

By adjusting the capillary coefficient of the ACC, k_{c12} , so that it is equal to k_{c2} in a double-sided hydrostatic pad, as shown in Fig. 2, and disregarding the applied load, the relationship between the initial clearances becomes $h_{11} = h_{21} = h_0$. Then, using the force equilibrium condition, the relationship between the resistance ratios of each pad is

$$\frac{(h_0 - \Delta h)^3}{k_{c12}} = \frac{(h_0 + \Delta h)^3}{k_{c2}} \quad (4)$$

$$k_{c12} = \frac{\pi}{6 \ln(r_o/r_i)} (h_{c1} - \Delta h_c)^3 = k_{c11} \left(1 - \frac{\Delta h_c}{h_{c1}}\right)^3$$

where r_i and r_o are the inner and outer radii of the capillary and Δh_c is the variation of the ACC clearance. From Eq. (4), the relationship between the ACC variation and the bearing clearance in a hydrostatic pad is

$$\frac{\Delta h_c}{h_{c1}} = \frac{2\Delta h/h_0}{1 + \Delta h/h_0} \quad (5)$$

From Eqs. (3) and (4), the capillary radius ratio of the ACC is

$$\frac{r_o}{r_i} = \exp\left(\frac{\pi \xi_0 h_{c1}^3}{6 \bar{B} h_0^3}\right) \quad (6)$$

Since the maximum values of Δh_c and Δh correspond to the output rate of the piezo actuator and the maximum controllable magnitude of error, the dimensional parameters and capillary coefficients of the ACC can be calculated from Eqs. (5) and (6).

4. Experimental Setup and Compensation Method

A front view of the tested hydrostatic table is shown in Fig. 3, and the experimental setup for the error compensation method is shown in Fig. 4. The table has six pairs of double-sided pads in the vertical direction and has three pairs of

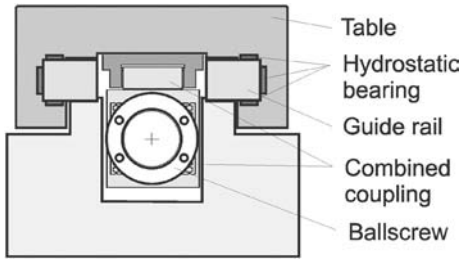


Fig. 3 Front view of a hydrostatic table

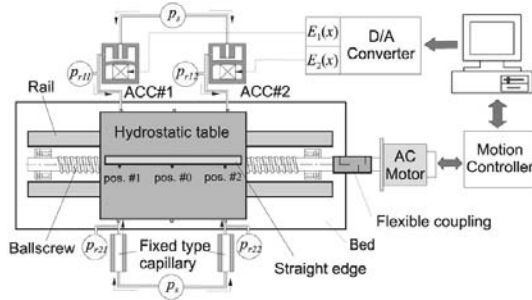


Fig. 4 Experimental setup to compensate for the motion errors

double-sided pads in the horizontal direction. The specifications of the hydrostatic table and ACC are listed in Table 1. A combined coupling consisting of a hydrostatic radial bearing and a mechanical hinge (Park et al., 1998) was placed between the hydrostatic table and the nut of the ballscrew to eliminate the ballscrew runout error. A DC servomotor (SC400, Pacific Scientific, 1 kW) was connected to the ballscrew with a flexible coupling, as shown in Fig. 4. The motor was controlled using a motion control board (PC/DSP, MEI, 16 bit) and a personal computer. Two ACCs were connected to both ends of the horizontal pad to compensate for the linear motion and yaw errors. The capillary coefficients of the ACCs were calibrated using a preloader placed under the piezo actuator so that they were equal to the coefficients of the fixed capillaries.

The micro-step response of the ACCs was tested by measuring the displacement of the leaf spring as a function of the input voltage to determine the minimum possible step. Then the micro-step response of the hydrostatic table with ACCs was tested by measuring the displacement

Table 1 Specifications of the hydrostatic table and ACC

Specifications	Horizontal pad	Vertical pad
Table width \times length B, L (mm)	30 \times 60	15 \times 60
Flow coefficient \bar{B}	1.657	2.437
Bearing clearance h_0 (μm)	47	49
Resistance ratio ξ	1	1
Table weight W (N)	0	107
Capillary coefficient k_c (mm^{-3})	1.7e-4	2.9e-4
Inner diameter of ACC r_i (mm)	4	4
Outer diameter of ACC r_o (mm)	16	16
Clearance of ACC h_c (μm)	77	92
Supply pressure P_s (Mpa)	1	
Dynamic viscosity of oil ν (cSt)	10.3 (40°C)	

of the table at positions 1 and 2 (refer to Fig. 4) according to the step command of the input voltages supplied to the ACC 1 and 2. The frequency bandwidth of the hydrostatic table with ACCs was also tested using the same method; in this case, the ACC input voltages were supplied using a function generator and a D/A converter. To determine the gains of the ACCs that were used for the compensation process, the step response of each ACC to a 1V/step command was tested and adjusted. All the responses were measured using capacitive sensors (Microsense 3401, ADE).

The error compensation process was designed as follows. First, the gains of the ACCs were adjusted using the previously tested step response characteristics. Next, the linear and angular motion errors of the feed table were measured using a laser interferometer (5528A, HP). Then appropriate linear and angular compensation coefficients K_z and K_θ were selected through individual tests. Using the measured motion errors, adjusted gain, compensation coefficients, and Eq. (1), the input voltages were calculated and the appropriate excitation voltage was supplied to the ACCs. Since the compensation was performed using an open loop process, the motion accuracies were not sufficiently improved during just one cycle of the compensation process due to the hysteresis of the piezo actuator and the adjusting error of the

gains. Therefore, the compensation process was iterated until the motion accuracies did not further improve. The iterative compensation method, which effectively controls high repeatability systems such as a hydrostatic table, was applied to improve the efficiency of the successive iteration process.

In the tests, the motion error was measured five times, and an averaged value was used to decrease the influence of non-repeatable errors.

5. Discussion of the Experimental Results

5.1 Response characteristics of the ACC

The measured least-step response of the ACC is shown in Fig. 5(a). The response of the ACC was distinct up to 2.5 mV/step, which was the minimum output resolution from the D/A converter. Theoretically, this corresponded to 4.5 nm/step. However, owing to the hysteresis of the piezo actuator, the practically measured resolution was 3.3 nm/step, as shown in the figure. The measured least-step response of the table with ACCs is shown in Fig. 5(b). The response of the table was distinct up to 27 nm/step; however, the response time was not fast. The tested frequency bandwidth of the table with ACCs was 5.5 Hz, as shown in Fig. 6. The main reason for the decreased frequency bandwidth was likely the compressibility of the polyurethane tube that supplied

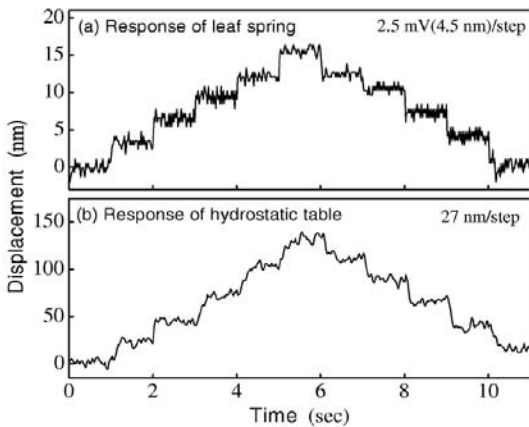


Fig. 5 Micro step response of the ACC and hydrostatic table

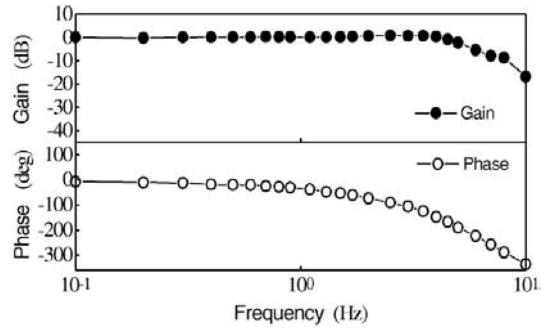


Fig. 6 Frequency bandwidth of the hydrostatic table with ACCs

oil to the hydrostatic table. In the motion error compensation tests, considering this low frequency bandwidth, the feed rate of the table v and distance prescribed by the compensation data Δx were fixed at 2 mm/s and 1.0 mm, respectively.

5.2 Adjusting the gain of the ACC

The step response characteristics before and after the ACC gains were adjusted are shown in Fig. 7. Fig. 7(a) gives the corresponding displacement of the table to 1 V/step of input voltage measured at the three positions described in Fig. 4. The gain of ACC 1 was less than that of ACC 2. The corresponding displacement of the table when the input voltage of ACC 2 was decreased to 0.94 V/step is shown in Fig. 7(b). The displacements at the three positions were almost the same. From these results, the gains of the ACCs

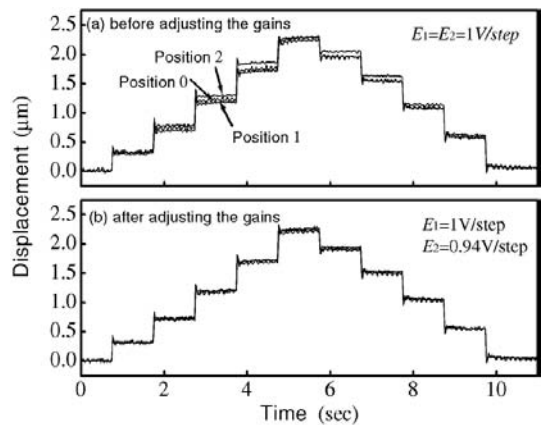


Fig. 7 Step response of the table according to the adjusted gain of the ACCs

were set to $G_1=2.083 \text{ V}/\mu\text{m}$ and $G_2=1.958 \text{ V}/\mu\text{m}$. Therefore, using G_1 , the maximum controllable range of the motion error within the maximum input voltage of 5 V was $2.4 \mu\text{m}$.

5.3 Compensation of the linear motion error

The measured motion errors of the tested hydrostatic table are shown in Fig. 8. The linear and angular motion errors were $1.70 \mu\text{m}$ and 1.21 arcsec , respectively, through a stroke of 250 mm.

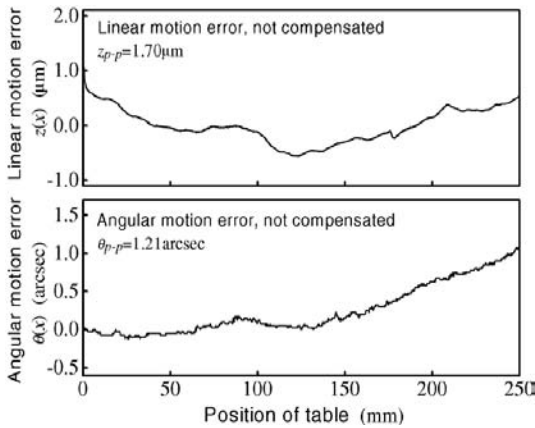


Fig. 8 Motion errors of the hydrostatic table before compensation

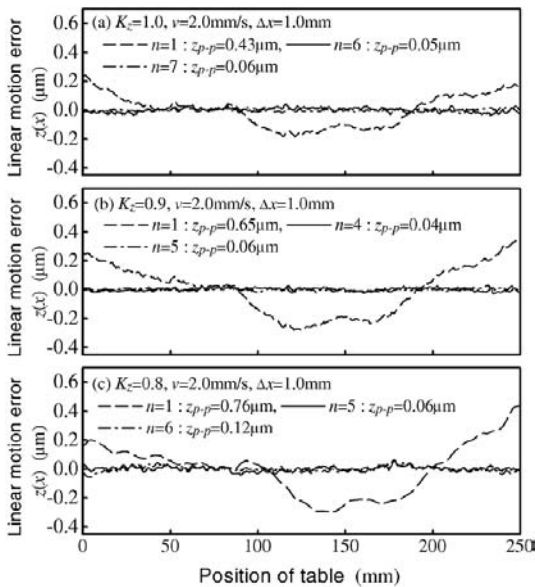


Fig. 9 Influence of the linear coefficient on the linear motion error compensation

The linear compensation coefficient K_z was varied between 1.0 and 0.8 to determine its influence on the motion compensation. The results are shown in Fig. 9. Even when $K_z=1.0$ (Fig. 10 (a)), which corresponded to the case when the measured error was directly converted into an input voltage for motion compensation, the linear motion error improved greatly over one compensation cycle. The remaining error was mainly due to the hysteresis of the piezo actuator and varied gains of the ACC. Also, the interference of the bending stiffness induced by the assembly error of the ballscrew had an effect on the system. As the number of iterations n increased, the linear motion accuracy continued to improve. The best result, $0.05 \mu\text{m}$, was obtained when $n=6$. When $K_z=0.9$, the best linear motion accuracy was obtained with the least number of iterations, $n=4$, as shown in Fig. 9 (b). When $K_z=0.8$, the value of the motion error and the number of iterations increased as compared to the $K_z=0.9$ case.

5.4 Simultaneous compensation of the motion errors

Using the results of the previous tests, simultaneous compensation of the linear and angular motion errors was attempted. The compensated results using $K_z=0.9$ for the linear coefficient and $K_\theta=0.9$ for the angular coefficient are shown in Fig. 10. After four iterative compensation cycles, the linear and angular motion errors were im-

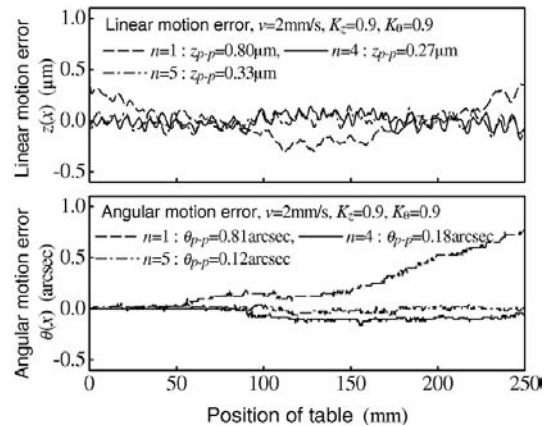


Fig. 10 Simultaneously compensated motion errors when $K_z=K_\theta=0.9$

proved to $0.27 \mu\text{m}$ and 0.18 arcsec . The angular motion accuracy continued to improve as the number of iterations increased. However, there was not a corresponding improvement in the linear motion accuracy. Comparison with the results shown in Fig. 9 shows that when only the linear motion error was corrected, the compensating characteristics were changed significantly by the interference of the input voltages used to correct the angular motion error. Also, as determined through additional tests on the effect of the angular coefficient K_θ , a change in K_θ did not improve the linear motion error. However, the value of the linear compensation coefficient did

affect the linear motion error.

The best results for the iterative motion compensation tests are shown in Fig. 11. When $K_z=0.6$ and $K_\theta=0.9$, the linear and angular motion errors improved to $0.12 \mu\text{m}$ and 0.20 arcsec , respectively, after three iteration cycles. The angular motion accuracy continued to improve as the number of iterations was increased, but the linear motion accuracy became worse. Thus, the linear and angular coefficients affected the corresponding motion errors independently.

The repeatability of the measured errors for the best case, when $K_z=0.6$, $K_\theta=0.9$, and $n=3$, is shown in Fig. 12. The data were measured five times and superimposed on each other in the figure. The repeatability, measured using the standard deviation $\pm 2\sigma$, was $\pm 0.04 \mu\text{m}$ and $\pm 0.05 \text{ arcsec}$ for the linear and angular errors, respectively. These values were mainly the result of the thermal effect of the oil, the measuring error of the laser interferometer, and the non-linearity of the ACCs.

6. Conclusions

In this study, the basic characteristics of ACCs were tested, such as the maximum controllable range, micro-step response, and available dynamic bandwidth. Simultaneous compensation of the linear and angular motion error of a hydrostatic table was performed using two ACCs. The experimental results showed that by using the ACCs, a motion error in the hydrostatic table within $2.4 \mu\text{m}$ could be corrected to a resolution of 27 nm , or about $1/90^{\text{th}}$ of the controllable range, with a frequency bandwidth of 5.5 Hz . Also, when the motion errors were corrected simultaneously, the linear and angular motion accuracies improved to $0.12 \mu\text{m}$ and 0.20 arcsec , or about $1/15^{\text{th}}$ and $1/6^{\text{th}}$ of the initial motion accuracies, respectively. These results confirm that the proposed motion error compensation method using ACCs improves the motion accuracy of a hydrostatic table very effectively.

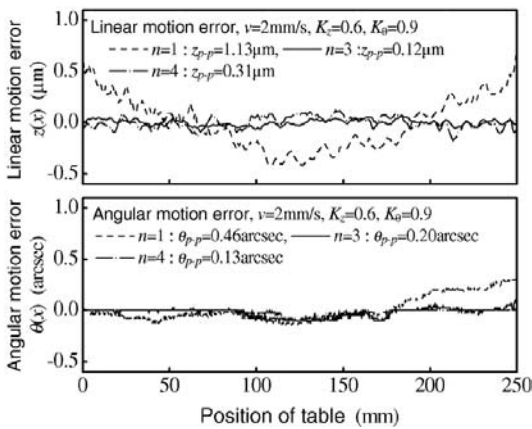


Fig. 11 Simultaneously compensated motion errors when $K_z=0.6$ and $K_\theta=0.9$

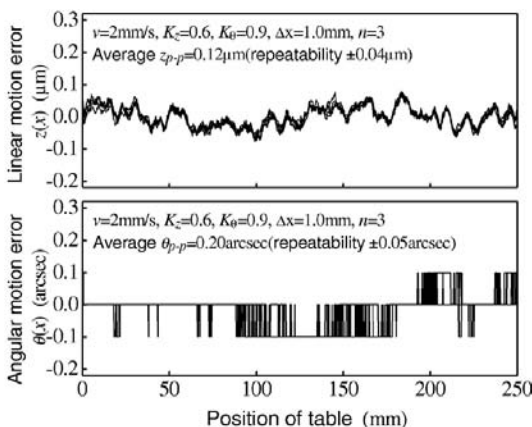


Fig. 12 Simultaneously compensated motion errors and their repeatabilities when $K_z=0.6$, $K_\theta=0.9$, $n=3$

References

- Aoyama, H., Watanabe, I., Akutsu, K. and Shimokohbe, A., 1988, "An Ultra Precision Straight Motion System (1st Report — Two Degrees of Freedom Control of Motion)," *J. of JSPE*, Vol. 54, No. 3, pp. 130~135.
- Aoyama, T., 1990, *Hydrostatic Bearing — Design and Applications*, Kougyojoushakai.
- Canbulut, F., Sinanoglu, C. and Yildirim, S., 2004, "Analysis of Effects of Sizes of Orifice and Pockets on the Rigidity of Hydrostatic Bearing Using Neural Network Predictor System," *KSME International Journal*, Vol. 18, No. 3, pp. 432~442.
- Hageman, L. A. and Young, D. M., 1981, *Applied Iterative Methods*, Academic Press, Inc.
- Mizumoto, H., Ariti, S., Kami, Y., Goto, K., Yamamoto, T. and Kawamoto, M., 1996, "Active Inherent Restrictor for Air-bearing Spindles," *Precision Engineering*, Vol. 19, No. 2/3, pp. 141~147.
- Park, C. H., Moriwaki, T. and Shamoto, E., 1998, "Coupling Mechanism for High Precision Feed Table with Ballscrew," *Int. Conf. on Manufacturing Milestones toward the 21st Century*, *JSME*, pp. 139~144.
- Sharma, S. C., Jain, S. C. and Bharuka, D. K., 2002, "Influence of Recess Shape on the Performance of a Capillary Compensated Circular Thrust Pad Hydrostatic Bearing," *Tribology International*, Vol. 35, pp. 347~356.